Area Model and Dimensioning Guidelines of Multisource Energy Harvesting for Nano–Micro Interface

Raul Gomez Cid-Fuentes, *Student Member, IEEE*, Albert Cabellos-Aparicio, and Eduard Alarcón, *Member, IEEE*

***Abstract*—Multisource energy harvesters are a promising, robust alternative to power the future Internet of Nano Things (IoNT), since the network elements can maintain their operation regardless of the fact that one of its energy sources might be temporarily unavailable. Interestingly, and less explored, when the energy availability of the energy sources present large temporal variations, combining multiple energy sources reduce the overall sparsity. As a result, the performance of a multiple energy harvester powered device is significantly better compared to a single energy source even if they harvest the same amount of energy. In this context, a framework to model and characterize the area for multiple source energy harvesting (EH) powered systems is proposed. This framework takes advantage of this improvement in performance to provide the optimal amount of energy harvesters, the requirements of each energy harvester, and the required energy buffer capacity, such that the overall area or volume is minimized. On top of these results, self-tunable energy harvesters are explored as a solution and compared to multisource EH platforms. As the results show, by conducting a joint design of the energy harvesters and the energy buffer, the overall area or volume of an EH powered device can be significantly reduced.**

***Index Terms*—Area optimization, energy-erlang, energy harvesting, multi-source harvesting, nanonetworks, self-tunable harvesting.**

I. Introduction

NANOTECHNOLOGY is providing a new set of tools to the engineering community to integrate communicating nanosensors. By means of communication, these nanosensors will be able to achieve complex tasks in a distributed manner [2]. The resulting nanonetworks will enable unique applications. For the time being, the communication options for nanosystems are very limited due to large constraints that these nanosensors face with regard to energy availability.

Recent advancements in electronics [2], [3] have pointed out that energy harvesting (EH) is a firm candidate as the key enabling technology in the development of nanonetworks with perpetual character. These upcoming networks show unique properties not only because of ultra-low power constraints but also because of the fact that the energy state is time varying. That is, the energy buffer (e.g., a supercapacitor or a battery) is constantly charging and discharging in a random manner [4]. For this reason, one of the main challenges in the design of such devices lies in the dimensioning of both the EH and energy buffer units [4]. Considering both subsystem units to be sufficiently large solves undesired interruptions during the normal operation of the nanosensor and, accordingly, on the nanonetwork. However, this comes at the cost of precluding desirable miniaturization of the nanosensors, caused by the relatively small power densities of existing ambient energy sources and low energy density of energy buffers [5], [6]. As an example, in order to harvest 0.2-mW vibrational energy and to store 1 J of energy, an energy harvester of approximated 1 cm^2 and an energy buffer of approximated 2 cm^3 would be required.

Recently, multisource energy harvesters are gaining interest as a robust alternative to power wireless sensors [7]. To implement multisource energy harvesters, there appear two feasible approaches. On the one hand, these can be implemented through platforms which combine a few number of energy harvesters, each devoted to each source of energy [7]–[9]. On the other hand, self-tunable approaches permit tuning their oscillating frequency, therefore enabling multiband capabilities to harvest energy from multiple energy sources [10], [11].

These platforms are more robust than the single-source ones. Indeed, if a certain energy source renders unavailable for a certain time period, due to the time asynchronicity among energy sources, the sensor node can still maintain its normal operation. An additional, but less explored, advantage of heterogeneous multiple source energy harvesters, which aids the miniaturization of the sensor nodes, is that when the ambient energy presents large temporal variations (i.e., the harvested power randomly varies over a wide range during time), the combination of multiple statistically independent energy sources lowers the sparsity of the overall energy which is harvested. This causes that devices, which are powered by multisource energy harvesters, show lower outage probabilities in contrast to single-source configurations. Equivalently, the requirements in terms of energy buffer capacity can be relaxed while maintaining the same performance. As an example, Fig. 1 shows three wireless motes that implement one, two, or four energy harvesters, which occupy the same overall area in a chip-like planar implementation.

Manuscript received February 23, 2015; revised May 01, 2015; accepted May 14, 2015. Date of publication June 01, 2015; date of current version January 20, 2016. This work was supported in part under an AGAUR FI-DGR grant and in part by the Spanish Science and Technology Ministry under National Project DPI2013-47799-C2-2-R.

The authors are with the NaNoNetworking Center in Catalunya (N3Cat), Universitat Politècnica de Catalunya (UPC), 08034 Barcelona, Spain (e-mail: rgomez@ac.upc.edu; acabello@ac.upc.edu; eduard.alarcon@upc.edu).

Digital Object Identifier 10.1109/JIOT.2015.2440176

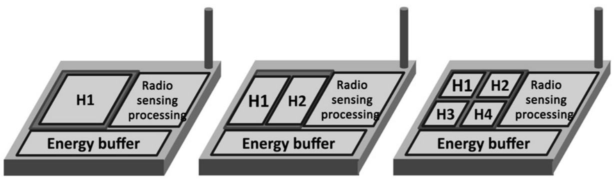

Fig. 1. Multisource EH enabled nano–micro interface. Increasing the number of sources reduces the efficient area for harvesting but maximizes the probability of finding an active energy source.

In this paper, we present an analytical framework to model the overall occupied area by the EH and energy buffer units. In particular, this model accounts for the requirements and capabilities of the wireless mote, and is useful to provide: 1) the optimal number of energy harvesters; 2) their size; and 3) the energy buffer capacity, such that the overall area of the wireless communicating device is minimized, while still meeting the user-defined requirements of the communications unit. On top of these results, we explore the capabilities of self-tunable energy harvesters as a feasible alternative to multisource platforms [10]. In this context, we evaluate their performance in terms of harvested power and compare it to the performance of multisource EH platforms.

To evaluate the provided model, we focalize on the design of the nano–micro interface [12]. This network element stems as the interface between the nanonetwork and the macroscale network. As such, nano–micro interfaces show larger requirements in terms of computation and communications capabilities and, therefore, these systems present larger power consumption as well as overall size. Notice, however, that this model can be scaled down to the size of a nanosensor, by assuming the detailed constraints of such devices.

This framework shows that harvesting energy from multiple sources by using either multisource platforms or self-tunable energy harvesters provides significant improvements in energetically sparse scenarios. These improvements, jointly considered with an optimal dimensioning of the energy buffer, will pave the way to smaller energy management units and, therefore, actual miniaturization of eventual nanonetworking devices. This paper is structured as follows. In Section II-A, we present the sparse energy sources. In Section III, we compare the performance of single-source to multisource energy harvester powered devices. In Section IV, we present the circuit area model to be optimized, while in Section V, we evaluate this model in a particular case. In Section VI, we explore the capabilities of self-tunable energy harvesters. Finally, in Section VII, we conclude our work.

II. Overview

In this section, we overview the properties of the environmental energy and define the metrics to evaluate the results of this work.

A. Sparse Energy Sources

Ambient energy is generally generated by the aggregation of an extensive number of physical entities which simultaneously radiate power [5]. Then, the random contribution of each entity, in both magnitude and time duration, entails a time-varying character in the aggregated power.

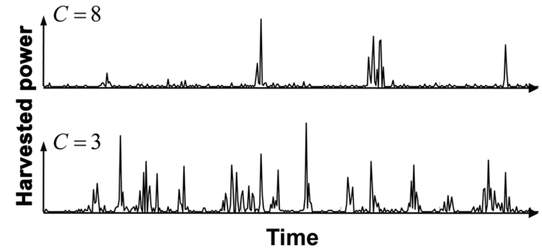

Fig. 2. Harvested power from a sparse ambient source of peak power to average power ratio of (upper) $C = 8$ and (lower) $C = 3$.

Accordingly, we refer to any physical phenomena which produces an aggregated power in a sparse, time-varying manner, such that this power cannot be known or estimated and the magnitude of the instantaneous power falls within a wide range, as a sparse energy source. In fact, sparse energy sources are present in a wide variety of physical phenomena. Among others, acoustic energy, mechanical, vibrational, or RF energy [13]–[15] are considered representative examples of such sources, when considering a large time scale.

In this work, we propose the peak power-to-average power ratio as a metric to enable the comparison of performance of ambient energy sources. This metric is given by

$$C = \frac{P_{\text{peak}}}{P_H} \tag{1}$$

where P_{peak} is the average peak power and P_H refers to the average harvested power. Fig. 2 shows examples of two random energy sources with different peak power to average power ratio ($C = 8$ and $C = 3$). As it is shown, energy sources with large peak power-to-average power ratios are characterized by short but powerful bursts of energy, while leaving large inter-burst times where the available energy is far below the average value. On the contrary, energy sources with low values of this metric are characterized by being more constant and predictable.

B. Evaluation Metrics

We use the energy utilization as a main metric to relate the occupied area of an energy harvester, its harvestable power, and the required performance of the nano–micro interface. The energy utilization provides a link between the energy model, the environmental harvested power, the network requirements, and the energy buffer capacity. This is defined as

$$\rho_e = \frac{P_C}{P_H} \tag{2}$$

where P_H is the harvested power and P_C stands for the required power to perform a certain application. The energy utilization is evaluated in the Energy–Erlang units [4].

Second, we use the energy outage probability p_{out} as a metric to evaluate the performance of the nano–micro interface. The energy outage is defined as the time interval during which the device node does not have enough stored energy, and thus its operation is temporarily interrupted.

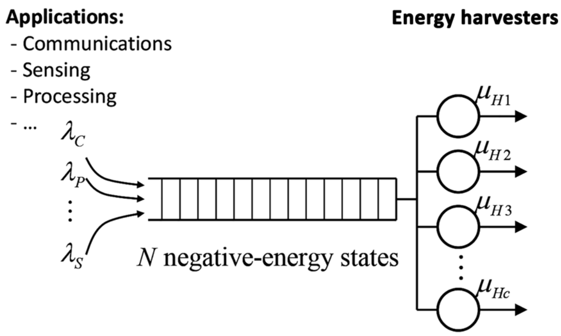

Fig. 3. Negative energy queue model.

III. Multiple Source Energy Harvesters

Multisource energy harvesters are able to combine the energy from multiple energy sources. This reduces the chances that the nano–micro interface is in a deep energy fading, where it is not able to harvest energy for a significant amount of time, since whenever an energy source is faded, any other energy source can be supplying energy. In other words, combining independent energy sources, the sparsity of the overall process is reduced and thus the energy fadings are potentially reduced, as well. In this section, we provide a model for multisource energy harvester platforms and evaluate the improvement on performance that using multiple EH platforms has when contrasted to single harvester platforms.

A. Energy Model

In order to evaluate the performance, we use the negative energy queue model [4], which is shown in Fig. 3. This Markov-based model is similar to other existing energy models for EH [16]–[19]. However, as it is shown, this model pursues to model an EH powered nano–micro interface as a classical communications queue, i.e.: 1) the stability condition must be $\rho_e < 1$; 2) the idle state is defined as the state of having an empty queue; and 3) the loss of communication is assigned to a full queue.

This model considers that the arrivals of this queue are generated by the set of applications of the nano–micro interface node, i.e., every time an application spends one unit of energy, it generates an arrival of negative energy. Each kind of application has an associated generation rate in power units (e.g., λ_C for communications, λ_P for processing, and λ_S for sensing). On the other hand, each harvester has an associated service time, $T_H = E_s/\mu_H$, which is the time that this EH unit needs to process one negative energy packet, where E_s is the energy of a negative energy packet and μ_H the EH rate in power units. We find that this time is characterized by a random variable defined as

$$t_H \equiv \text{time s.t.} \int_{t_H} P_H(t)dt = E_s. \tag{3}$$

Thus, the number N of negative energy states is related to the energy buffer capacity C_B as

$$N = \frac{C_B}{E_s}. \tag{4}$$

Additionally, if, at a certain time t_k, the queue has L_k negative energy packets, then the energy state s_k at the energy buffer is given by

$$s_k = C_B - L_k E_s. \tag{5}$$

This models brings significant benefits to model multisource energy harvesters. In particular, the negative-energy queue model is able to easily handle multiple energy harvesters, by connecting them in parallel, such as a communication queue with multiple servers (e.g., M/M/c/N, M/G/c/N, and G/G/c/N).

In order to exemplify this, if we assume a single-source energy harvester, the outage probability can be easily calculated by means of queue theory on M/G/1/N

$$p_{\text{out}} = P_N = 1 - \frac{1}{\pi_0 + \rho_E} \tag{6}$$

where π_0 refers to the probability that there are zero negative-energy packets left within the queue right after the last negative-energy packet was processed by the energy harvester. As such, it is only required to estimate the probability of having a depleted queue. In particular, π_0 is found as a solution for

$$\pi_n = \sum_{n=0}^{N-1} \pi_j p_{jn}, \quad 0 \leq n \leq N-1 \text{ and } \sum_{n=0}^{N-1} \pi_n = 1 \tag{7}$$

where equivalent to π_0, π_n refers to the probability that there are n negative-energy packets left and p_{jn} stands for the state transition probability of remaining negative-energy packets from the state j to the state n, considering each state right after a negative-energy packet has been processed by the energy harvester.

B. Performance of a Multiple Source Energy Harvester

We focus on the nano–micro interface to evaluate the provided model. A nano–micro interface is expectedly larger than the remaining nanosensors, since these must operate as a network interface between the nanonetwork and the macroscale environment. For these devices, we have considered an average communications rate of $\lambda_c = P_C = 100$ μW. Then, we have considered each negative energy packet to be of 10 μJ. Finally, we have set the overall harvesting rate $N\mu_H = P_H = P_C/\rho$, where ρ_e has been set as an evaluation parameter. Therefore, each harvester harvests an average power of $P_C/\rho_e N$. These EH rates can be achieved by means of vibrational harvesters [5].

In order to generate the sparse energy sources, we have approximated the ambient energy by a random process generated by exponentially distributed energy bursts of power $P_H C/N$, with an inter-burst time of $0.1/C$ s. An exponentially distributed random process has been chosen as it presents the largest entropy, thus estimating the worst case [13].

Figs. 4 and 5 compare the improvement over p_{out} that using multiple harvesters has as a function of the energy buffer capacity C_B for a peak power-to-average power ratio of $C = 10$ and $C = 100$, respectively. These results have been obtained by assuming in the negative energy queue model $\rho_e = 0.9$. As it is shown, there is a clear improvement, since varying from one

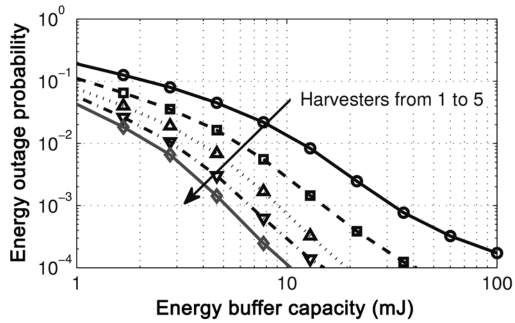

Fig. 4. Energy outage probability as a function of the energy buffer capacity. $\rho_E = 0.9$ E2 and $C = 10$.

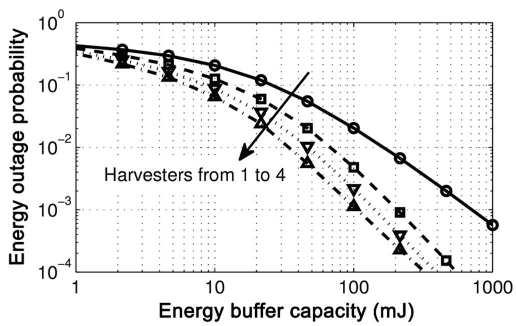

Fig. 5. Energy outage probability as a function of the energy buffer capacity. $\rho_E = 0.9$ E2 and $C = 100$.

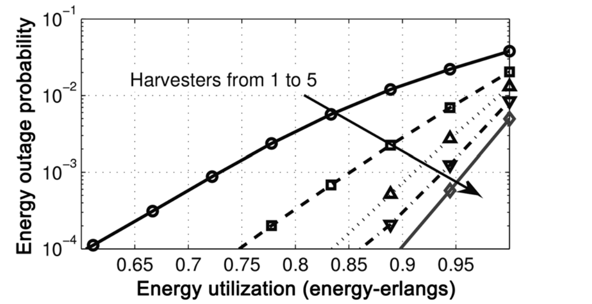

Fig. 6. Energy outage probability as a function of the energy utilization. $C_B = 10$ mJ and $C = 10$.

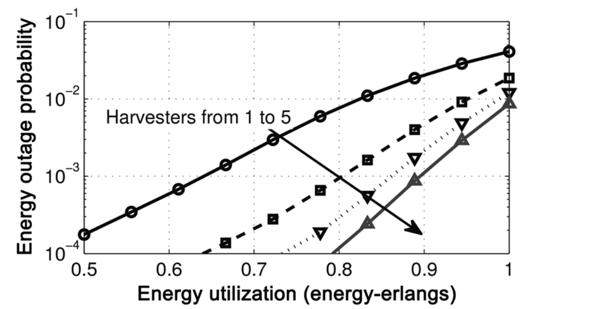

Fig. 7. Energy outage probability as a function of the energy utilization. $C_B = 100$ mJ and $C = 100$.

to five harvesters, the energy buffer capacity can be reduced from 30 to just 5 mJ and from 600 to just 100 mJ, while still maintaining $p_{\text{out}} < 10^{-3}$.

In addition to this, Figs. 6 and 7 compare this improvement as a function of the ρ_e for peak power-to-average power ratios of $C = 10$ and $C = 100$, respectively. In order to obtain these results, the energy buffer capacity has been set to $C_B = 10$ mJ in Fig. 6 and to $C_B = 100$ mJ in Fig. 7. As it is shown, multisource energy harvesters are able to provide similar performance, but at larger ρ_e values and, therefore, requiring smaller EH area.

As a result, we observe that multisource energy harvesters can help reducing both the energy buffer capacity and the EH requirements, while still providing the required performance.

IV. Circuit Area Model

As seen in the previous section, additional energy harvesters have a positive impact upon the performance. Nonetheless, this technique produces a nonnegligible area overhead, since each energy harvester requires some additional circuitry and separation space.

An additional compromise is that low values of ρ_e help reducing the energy buffering capacity at the cost of proportionally increasing the EH requirements.

These compromises motivate a framework for circuit area optimization which considers the user-defined requirements, the area overhead of multiple harvesters, and the energy buffer capacity. In order to do so, we first relate the required power, harvesting power, number of harvesters and energy buffer capacity, which are able to achieve the required performance in energy outage probability, through the energy model presented in Section III. Afterward, this is translated into circuit area by means of the following model.

We then define the overall area of the system as

$$A_{\text{TOTAL}} = A_H + A_B + A_A \tag{8}$$

where A_H refers to the area of the harvesting unit, A_B stands for the area of the energy buffer unit, and A_A is the area of the applications units (i.e., processing, sensing, and communications unit). In particular, since A_A is fixed and provided by a certain application, A_A is not considered in the following circuit area optimization.

A. *Area of the EH Unit*

The area of the harvesting unit depends on mainly two factors, the number of energy harvesters and the power that these aim to harvest. As shown in [5], the ambient power is generally characterized by a given power density. As such, the overall area is expectedly proportional to the desired power to be harvested. Alternatively, integrating more than one energy harvester requires additional circuitry, which increases the eventual size of the unit. In this work, we linearly approximate the area of the EH unit in terms of the number of energy harvesters and desired power rate

$$A_H = A_{H0} + A_{HN}N_H + A_{HP}P_R/\rho_e \tag{9}$$

where A_{H0} refers to a constant area, A_{HN} to the partial contribution of A_H with respect to the number N_H of energy

TABLE I
VALUES USED IN THE OPTIMIZATION FRAMEWORK

Parameter	Value	Units
A_{H0}	0.01	cm^2
A_{NH}	.01	cm^2
A_{NP}	6.66	$\mathrm{cm}^2\ \mathrm{mW}^{-1}$

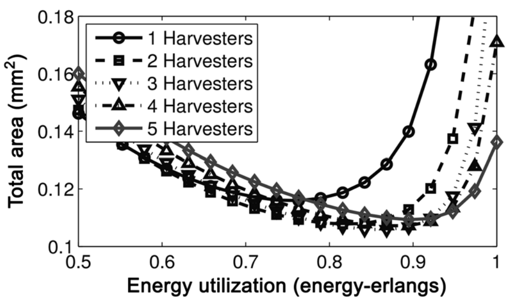

Fig. 8. Overall area in terms of the energy utilization. $C = 10$.

harvesters, and A_{HP} to the partial contribution of A_H with respect to the required power P_H.

The considered values in this work are shown in Table I. These correspond to reasonable values that have previously been reported [5].

B. Area of the Energy Buffer

In line with recent advancements in energy buffering [6], each technology presents an associated energy density. In this context, we have considered consistent values for this density of $D_B = 2\ \mathrm{J/cm}^3$ and a fixed height of 1 cm. Similar to A_H, we may linearly approximate the overall area of the energy buffer as

$$A_B = A_{B0} + C_B D_B \tag{10}$$

where A_{B0} is a fixed area overhead and C_B is the required capacity of the energy buffer in millijoules units.

V. EVALUATION OF THE AREA MODEL

In order to optimize the area, we have simulated the nano–micro interface through the same energy model as described in the previous sections. Then, we have assumed a tolerable performance of a wireless device, when its energy outage probability is below $p_{\mathrm{out}} = 10^{-4}$.

Fig. 8 shows the overall occupied area for the joint EH and energy buffer unit, such that the user-defined requirements in terms of output power and energy outage probability are met. This area corresponds assuming that the environmental energy is characterized by a peak power-to-average power ratio of $C = 10$. As it is shown, the overall area shows an optimal minimum for $\rho_e = 0.87$ E2. This is due to the fact that for fixed values of power requirements, a large energy utilization ratio reduces the amount of harvested energy, therefore reducing the size of the energy harvester. However, this reduction in the energy harvester comes at the price of increasing the size of the energy buffer.

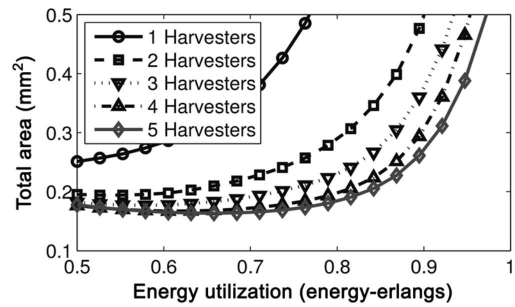

Fig. 9. Overall area in terms of the energy utilization. $C = 100$.

TABLE II
COMPONENT REQUIREMENTS

C	Parameter	Value	Units
10	Harvesters	4	—
	Area harvester (total)	7.7	mm^2
	P_H (each)	27.7	µW
	Area energy buffer	3	mm^2
	Capacity energy buffer	15	mJ
100	Harvesters	5	—
	Area harvester (total)	8.3	mm^2
	P_H (each)	40	µW
	Area energy buffer	5	mm^2
	Capacity energy buffer	25	mJ

Similarly, Fig. 9 shows the results of the circuit area optimization when considering the same system requirements, but assuming a peak power to average power of $C = 100$. As it is shown, an increase in this ratio enlarges the size of the overall area, regardless of the number of energy harvesters and their operation point. This increase is caused by the fact that the nano–micro interface runs on the stored energy for a longer time. In this case, it is found that increasing the number of energy harvesters shows a significant benefit, since the sparsity of the energy is reduced. In particular, the minimum area is found at a $\rho_E = 0.66$ E2, considering five energy harvesters. The outcomes of this design, which are required for the EH unit and an energy buffer to minimize the area, can be found in Table II for both cases.

VI. SELF-TUNABLE MULTIBAND ENERGY HARVESTERS

In case that the considered energy sources are of the same type and the difference among them is that each is produced at a different frequency band, self-tunable energy harvesters emerge as an encouraging alternative to multisource platforms. These devices have the property of tuning their oscillating frequency over a wide range to adapt it to the frequency band of the harvestable energy [10].

This technology aims to provide a much higher performance compared to independent multisource platforms in cases where the ambient energy is very sparse and the frequency bands are uncorrelated to each other. In this case, a single energy harvester can generate more power than small energy harvesters. However, this improvement compared to multisource platforms is not always achieved because of two main reasons. On the one hand, when the different bands generate power simultaneously,

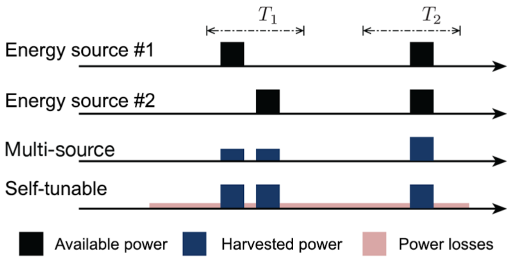

Fig. 10. Comparison between multisource and self-tunable platforms.

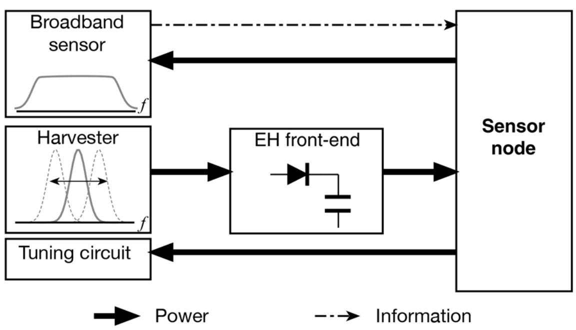

Fig. 11. Generic block diagram of an EH powered device that employs a self-tunable energy harvester.

self-tunable energy harvesters can only tune one of the frequencies, thus disregarding the other bands. On the other hand, a similar concept to cognitive-radio communications [20], these devices must implement spectrum sensing techniques to detect which frequency band generates a larger amount of power, therefore requiring power to generate power.

To exemplify this, consider the time diagram shown in Fig. 10. In this figure, two Internet of nano things (IoNT) platforms (one equipped with a multisource platform, and one equipped with a self-tunable harvester) harvest power from bands #1 and #2. We consider that both platforms integrate an energy harvester of the same overall occupied area. Therefore, the self-tunable energy harvester integrates a single energy harvester which can select the operating frequency band, whereas the multisource energy harvester is divided by two energy harvesters, one for each frequency band. Then, we observe that during the time T_1, both energy sources generate power at different times, whereas during T_2, the energy sources simultaneously generate power. As a result, the self-tunable energy harvester shows potential improvement during T_1 since it can harvest twice power, whereas the multisource platform scavenges more energy during T_2 since both harvest the same amount of power, while this does not require to spend power in sensing the environment.

In this section, we provide a generic model for a self-tunable energy harvester and compare their performance to multisource approaches as a function of critical factors which affect their performance.

A. *Self-Tunable Energy Harvester*

We show a generic model block diagram of a self-tunable energy harvester in Fig. 11. This is composed of four subunits, namely the broadband sensor, harvester, EH front-end, and tuning circuit. As this figure shows, the harvester is the only subunit which generates power, whereas the remaining units require power to realize their operation. We define the net harvested power as the net contribution of power generated by the harvester, broadband sensor, and tuning circuit

$$P_H = \eta P_{\mathrm{EH}}(t, B) - P_B - P_T \tag{11}$$

where η stands for the efficiency of the EH front-end, P_{EH} is the power generated in the harvester subunit, which is tuned at the band B, P_B refers to the required power from the broadband sensor to operate, P_T stands for the power which is consumed in the tuning circuit. As it follows, we briefly describe the operation of each unit.

1) Harvester: The tunable energy harvester stems as the key element in the EH unit. This is the only component that generates energy by converting environmental energy into electric current. This component has tunable properties, i.e., its oscillating frequency can be modified by adjusting its electrical parameters. Providing that this component generates energy, there is a direct relation between its occupied area and the power that it is able to harvest. As such, it is desired that this component occupies the largest area allocated for the EH unit. The harvested power is given by

$$P_{\mathrm{EH}}(t, B) = (S(t) * h(t, B))\, A_{\mathrm{eff}} \tag{12}$$

where S is the spectral power density of the available energy source, in power/area units, $h(t, B)$ stands for the transfer function of the harvester, which is tuned to the band B, and A_{eff} refers to the effective area of the harvester.

2) Broadband Sensor: In order to choose the optimal oscillating frequency of the energy harvester, a broadband sensor is integrated to detect most powerful band.These devices show remarkable properties to detect oscillations at a significantly wide frequency range. Unfortunately, they cannot be used as energy harvesters. As it is shown in Fig. 11, this unit requires a supply power to operate and to reports the sensed information. The nano–micro interface must integrate spectrum sensing tools to process this information to decide whether to retune the harvester. The power consumed by this unit P_B is assumed constant during the normal operation of the device.

3) Tuning Circuit: This circuit accommodates the natural frequency of the EH depending on the processed results retrieved by the sensed data of the broadband sensor. The basic element of this circuit is a capacitor. By selecting a capacitor voltage V_C, the natural frequency of the energy harvester is tuned to a different frequency. Recent studies show approximately linear dependency between the frequency and this voltage [10]. As such, the tuned band B is selected according to

$$B = k f_0 V_C \tag{13}$$

where k is a given constant, f_0 is the center frequency of the harvester, and V_C refers to the capacitor voltage Providing that the number of bands depends on the capacitor voltage, switching to additional bands requires additional voltage levels. Unfortunately, charging a capacitor to a higher voltage has

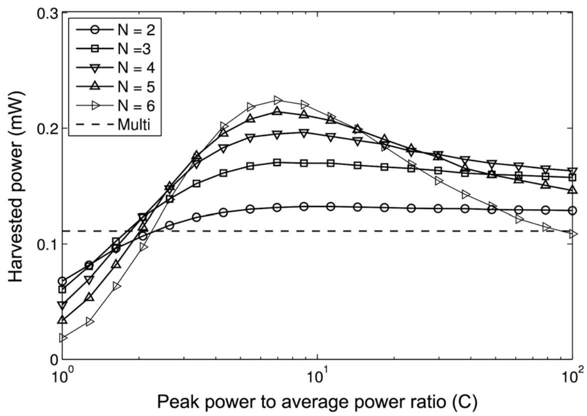

Fig. 12. Harvested power as a function of the peak power to average power ratio in self-tunable energy harvesters.

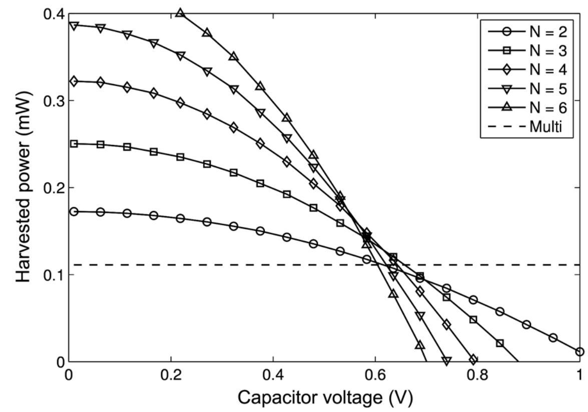

Fig. 13. Harvested power as a function of the capacitor voltage in self-tunable energy harvesters.

an associated quadratic loss of energy. Accordingly, the energy required to switch from one band to another is given by

$$E_{\mathrm{sw}} = \frac{1}{2} C (\Delta V_C)^2 \tag{14}$$

where ΔV_C refers to the difference between voltage levels.

4) EH Front-End: This unit is in charge of adapting the power which is generated by the energy harvester to generate a dc current which is delivered to the energy buffer and the remaining subsystem units of a nano–micro interface or a nanosensor. As a result of this power-processing operation, the actual power which is delivered to the device is always lower than that produced by the energy harvester [4]. This is generally referred to as the efficiency of the energy harvester.

B. Performance Evaluation

We evaluate the performance of a self-tunable energy harvester in terms of the average power which is able to generate. For this, we consider the energy balance at the energy harvester by calculating the generated power and the power losses derived from sensing the spectrum and retuning the harvester.

To derive the generated power, we have assumed that a self-tunable energy harvester occupies the same area as the optimized case in multisource EH platforms and is able to generate the same power. Alternatively, we have assumed that the power that the energy harvester consumes to sense the spectrum, to process this information and to tune the oscillating frequency of the energy harvester, referred to as P_{loss}, quadratically depends on the voltage range applied V_C to an equivalent capacity of $C_{\mathrm{eq}} = 1$ μF, which is a reasonable value as reported in [10]. The voltage applied at the capacitor linearly depends on the number of frequency bands, as shown in (13).

Fig. 12 shows the harvested power as a function of the peak power-to-average power ratio C for different number of available bands. In addition, we compare the results to the multisource energy platform which has been optimized in the previous section for $C = 10$ with four energy harvesters. In order to calculate these results, we have considered that the voltage difference to tune between consecutive bands is 0.5 V. As this figure shows, when the peak power-to-average power ratio increases, the power of the energy sources is more compacted in time. Then, the likelihood that two energy sources are generating power at the same time is reduced. This permits the energy harvester to maximize the harvestable energy, thereby showing a better performance than multisource energy harvesters. However, as this factor becomes large, the energy devoted to perform spectrum sensing and tuning the oscillating frequency gains significance, thus negatively impacting on the performance of the energy harvester. In addition, it is observed that the number of frequency bands plays an important role in the performance of the energy harvester. In fact, considering more energy bands improve the likelihood of a given band being active, but significantly increases the power losses.

Then, Fig. 13 shows the harvested power as a function of the applied voltage at the equivalent capacitor. In addition, we compare the results to the multisource energy platform which has been optimized in the previous section for $C = 10$ with four energy harvesters. To calculate these values, a peak power-to-average power ratio of $C = 10$ has been assumed. As it is shown, the applied voltage has a very strong impact on the performance of the energy harvester. In fact, as this voltage approaches zero, increasing the number of bands can provide a very large improvement compare to multisource EH platforms. As an example, using a self-tunable energy harvester to harvest from four bands generates almost three times the energy that an optimized multisource energy harvester with the same number of bands. However, as the required capacitor voltage increases, the performance of the energy harvester is being affected, therefore, showing equal performance at a capacitor voltage of approximately $V_C = 0.65$ V. This shows the need of sophisticated sensing schemes to minimize the power consumption.

Finally, we optimize the number of bands of a self-tunable energy harvester as a function of the peak power-to-average power ratio and capacitor voltage in Fig. 14. In addition, this performance is compared to the performance of multisource EH platforms. As this figure shows, regardless of the associated power losses of the EH unit, multisource EH platforms outperform self-tunable harvesters, in terms of outage probabilities, for moderately low values of C. Then, as

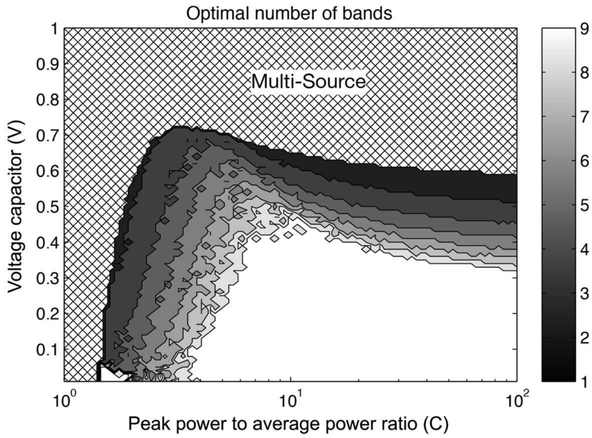

Fig. 14. Design space of self-tunable energy harvesters. Optimal number of bands as a function of the capacitor voltage and peak power-to-average power ratio.

this parameter increases, the effect of the capacitor voltage becomes significant. In particular, it is observed that a less number of bands show more robust performance in terms of both studied parameters, whereas considering a large number of bands requires low capacitor voltages and large peak power-to-average power ratios.

VII. Conclusion

Multisource EH is gaining popularity as an alternative to power nanonetworks. The benefits that this alternative provides when the ambient energy is largely time-variant is twofold: on the one hand, it provides robustness to the sensors and nano–micro interfaces, while on the other hand, the sparsity of the overall contribution is reduced, and thus its operation lifetime is improved. In this context, circuit area optimization, which considers both energy harvester and energy buffer and takes advantage of the improvement in performance of multiple source energy harvesters, has been addressed. As it has been shown, this joint effort can help reducing the overall area, thus enabling circuit area optimization to pursue a future miniaturization of the communicating devices toward the nanoscale. In addition, the performance of self-tunable energy harvesters has been compared to an optimized multisource energy harvester. Self-tunable harvesters have shown better performance especially when the presented environmental energy is very sparse. However, the operation of these devices requires sensing and computing tasks to actively select the optimal energy band.

References

[1] R. Cid-Fuentes, A. Cabellos-Aparicio, and E. Alarcon, “Circuit area optimization in energy temporal sparse scenarios for multiple harvester powered systems,” in *Proc. IEEE Int. Symp. Circuits Syst. (ISCAS)*, Jun. 2014, pp. 2486–2489.

[2] Y. Hu, Y. Zhang, C. Xu, L. Lin, R. L. Snyder, and Z. L. Wang, “Self-powered system with wireless data transmission,” *Nano Lett.*, vol. 11, no. 6, pp. 2572–2577, 2011.

[3] J. Jornet and I. Akyildiz, “Joint energy harvesting and communication analysis for perpetual wireless nanosensor networks in the terahertz band,” *IEEE Trans. Nanotechnol.*, vol. 11, no. 3, pp. 570–580, May 2012.

[4] R. Gomez Cid-Fuentes, A. Cabellos-Aparicio, and E. Alarcon, “Energy buffer dimensioning through energy-erlangs in spatio-temporal-correlated energy-harvesting-enabled wireless sensor networks,” *IEEE J. Emerg. Sel. Topics Circuits Syst.*, vol. 4, no. 3, pp. 301–312, Sep. 2014.

[5] S. Sudevalayam and P. Kulkarni, “Energy harvesting sensor nodes: Survey and implications,” *IEEE Commun. Surv. Tutorials*, vol. 13, no. 3, pp. 443–461, Third Quarter 2011.

[6] D. Pech *et al.*, “Ultrahigh-power micrometre-sized supercapacitors based on onion-like carbon,” *Nat. Nano*, vol. 5, no. 9, pp. 651–654, Sep. 2010.

[7] S. Bandyopadhyay and A. Chandrakasan, “Platform architecture for solar, thermal, and vibration energy combining with MPPT and single inductor,” *IEEE J. Solid-State Circuits*, vol. 47, no. 9, pp. 2199–2215, Sep. 2012.

[8] C. Park and P. Chou, “Ambimax: Autonomous energy harvesting platform for multi-supply wireless sensor nodes,” in *Proc. 3rd Annu. IEEE Commun. Soc. Sensor Ad Hoc Commun. Netw. (SECON)*, 2006, vol. 1, pp. 168–177.

[9] A. S. Weddell, M. Magno, G. V. Merrett, D. Brunelli, B. M. Al-Hashimi, and L. Benini, “A survey of multi-source energy harvesting systems,” in *Proc. Des. Autom. Test Eur. Conf. Exhib. (DATE)*, 2013, pp. 905–908.

[10] C. Eichhorn, R. Tchagsim, N. Wilhelm, and P. Woias, “A smart and self-sufficient frequency tunable vibration energy harvester,” *J. Micromech. Microeng.*, vol. 21, no. 10, p. 104003, 2011.

[11] S. Jo, M. Kim, and Y. Kim, “Passive-self-tunable vibrational energy harvester,” in *Proc. Int. Solid-State Sens. Actuators Microsyst. Conf. (TRANSDUCERS)*, Jun. 2011, pp. 691–694.

[12] I. Akyildiz and J. Jornet, “The internet of nano-things,” *IEEE Wireless Commun.*, vol. 17, no. 6, pp. 58–63, Dec. 2010.

[13] M. Win, P. Pinto, and L. Shepp, “A mathematical theory of network interference and its applications,” *Proc. IEEE*, vol. 97, no. 2, pp. 205–230, Feb. 2009.

[14] S. Chalasani and J. Conrad, “A survey of energy harvesting sources for embedded systems,” in *Proc. IEEE Southeastcon*, 2008, pp. 442–447.

[15] A. Hajati, S. Bathurst, H. Lee, and S. Kim, “Design and fabrication of a nonlinear resonator for ultra wide-bandwidth energy harvesting applications,” in *Proc. IEEE Int. Conf. Micro Electro Mech. Syst. (MEMS)*, Jan. 2011, pp. 1301–1304.

[16] R. G. Cid-Fuentes, A. Cabellos, and E. Alarcon, “Energy harvesting enabled wireless sensor networks: Energy model and battery dimensioning,” in *Proc. 7th Int. Conf. Body Area Netw. (BODYNETS)*, Sep. 2012, pp. 131–134.

[17] R. Rajesh, V. Sharma, and P. Viswanath, “Information capacity of energy harvesting sensor nodes,” in *Proc. IEEE Int. Symp. Inf. Theory*, Jul. 31/Aug. 5, 2011, pp. 2363–2367.

[18] O. Ozel, K. Tutuncuoglu, J. Yang, S. Ulukus, and A. Yener, “Transmission with energy harvesting nodes in fading wireless channels: Optimal policies,” *J. Sel. Areas Commun.*, vol. 29, pp. 1732–1743, Sep. 2011.

[19] M. Gorlatova, A. Wallwater, and G. Zussman, “Networking low-power energy harvesting devices: Measurements and algorithms,” in *Proc. IEEE INFOCOM*, Apr. 2011, pp. 1602–1610.

[20] D. Cabric, A. Tkachenko, and R. Brodersen, “Spectrum sensing measurements of pilot, energy, and collaborative detection,” in *Proc. IEEE Military Commun. Conf.*, Oct. 2006, pp. 1–7.

Raul Gomez Cid-Fuentes (GSM’12) received the B.Sc. and M.Sc. degrees in telecommunications engineering from the Universitat Politècnica de Catalunya (UPC), Barcelona, Spain, both in 2011, and is currently working toward the Ph.D. degree in nanonetworking at UPC.

He has been a Visiting Researcher with the Geneys Laboratory, Northeastern University, Boston, MA, USA (2014), and with the Broadband Wireless Networking Laboratory, Georgia Institute of Technology, Atlanta, GA, USA. His research interests include energy-harvesting enabled wireless networks, wireless RF power transmission, and nanonetworks

Albert Cabellos-Aparicio received the B.Sc., M.Sc., and Ph.D. degrees in computer science engineering from the Technical University of Catalonia (UPC), Barcelona, Spain, in 2001, 2005, and 2008, respectively.

In September 2005, he became an Assistant Professor with the Department of Computer Architecture and as a Researcher with the Broadband Communications Group. In 2010, he joined the NaNoNetworking Center in Catalunya, UPC, where he is the Scientific Director. He has been a Visiting Researcher with Cisco Systems and Agilent Technologies and a Visiting Professor with the Royal Institute of Technology (KTH), Stockholm, Sweden, and the Massachusetts Institute of Technology (MIT), Cambridge, MA, USA. He founded the LISPmob open-source initiative along with Cisco. He has participated in several national (Cicyt), EU (FP7), USA (NSF) and industrial projects (Samsung and Cisco). He has given more than ten invited talks (MIT, Cisco, INTEL, MIET, Northeastern Univ., etc.). He has coauthored more than 15 journal and 40 conference papers. His research interests include future architectures for the Internet and nano-scale communications.

Dr. Cabellos-Aparicio is an Editor of the *Elsevier Journal on Nano Computer Network* and founder of the ACM NANOCOM conference, the IEEE MONACOM workshop and the N3Summit. He was the recipient of a full scholarship from UPC in 2004 to carry out his Ph.D. studies with the Department of Computer Architecture.

Eduard Alarcón (S'96–M'01) received the M.Sc. and Ph.D. degrees in electrical engineering from the Technical University of Catalonia (UPC), Barcelona, Spain, in 1995 and 2000, respectively.

He became an Associate Professor with UPC in 2001, and has been a Visiting Professor with the University of Colorado at Boulder, Boulder, CO, USA (2003, 2006, and 2008) and with the Royal Institute of Technology (KTH), Stockholm, Sweden (2011). He has given 30 invited lecturers and tutorials worldwide. He has coauthored more than 300 scientific publications and 8 book chapters. He holds eight patents. He has been involved in different national, EU, and US R&D projects. His research interests include the on-chip energy management circuits, energy harvesting and wireless energy transfer, nanocommunications, and small satellites.

Dr. Alarcón is the Vice President of the IEEE CAS Society. He was elected a member of the IEEE CAS Board of Governors (2010–2013) and was the IEEE CAS Society Distinguished Lecturer. He is the Co-Editor of 6 journal special issues, 8 conference special sessions, TPC Co-Chair and TPC member of 30 IEEE conferences, and Associate Editor for the IEEE TRANSACTIONS ON CIRCUITS AND SYSTEMS–I: REGULAR PAPERS, the IEEE TRANSACTIONS ON CIRCUITS AND SYSTEMS–II: EXPRESS BRIEFS, *Journal on Emerging and Selected Topics in Circuits and Systems, Journal on Low-Power Electronics*, and *Nano Communication Networks*. He was the recipient of the Best Paper Award of the IEEE MWSCAS98.